JOURNAL OF GUIDANCE, CONTROL, AND DYNAMICS
Vol. 24, No. 1, January–February 2001

Deferred-Correction Optimal Control with Applications to Inverse Problems in Flight Mechanics

Carlo L. Bottasso* and Andrea Ragazzi†
Politecnico di Milano, 20158 Milano, Italy

We develop a numerical procedure for the inverse simulation of flight, formulated as an optimal-control problem. The resulting method is general and applicable to both fixed and rotating wing vehicles. We use the *p* version of the finite-element-in-time method, equipped with a deferred-correction acceleration technique for achieving the desired level of accuracy in the response at a low computational cost. We test our numerical procedures with the aid of some representative simulations.

Introduction

WE study the inverse simulation of flight for both fixed and rotating wing aircrafts. The problem is formulated by using optimal-control theory. Numerical procedures for inverse problems in flight mechanics have been presented in Refs. 1–8. Among these, Refs. 3 and 8 use optimal-control theory for studying the problem of inverse simulation, and they are therefore closely related to the present work.

Our numerical approach is based on a direct, finite-element discretization of the classic variational principle of optimal control. This idea was first proposed in Ref. 9. References 10–15 detail the application of this technique to all the major aspects of optimal control, including control inequality constraints, state constraints, unknown final time, and multiphase problems, and they present interesting applications of this technique.

We proved in Ref. 16 that this procedure is equivalent to the use of a certain class of global, implicit Runge–Kutta (RK) schemes. This result is valid for the *p* version of the method, that is, for arbitrarily high order. Similar results were derived in Ref. 17 for initial value problems. The analysis shows that the quadrature rule used for evaluating the integrals in the weak form plays a major role, in practice determining the algorithmic properties of the resulting finite-element-in-time (FET) scheme. Using the Gauss–Legendre, Lobatto, and Radau–Left quadrature rules, one obtains FETs that correspond to the Kuntzmann–Butcher (Gauss), Lobatto IIIB, and Radau IA RK schemes, respectively. The first two are effective solvers for boundary-value problems. In fact, the publicly available codes COLNEW[18] and ACDC[19] are respectively based on Gauss and Lobatto IIIA RK schemes.

Notwithstanding the equivalence of the methods, we believe there is still a motivated desire to look at FETs. For example, some new developments such as a posteriori error estimation might be easier to accomplish in one framework rather than another.[20] Furthermore, additional insight can usually be obtained by a unified view of any given problem.

The solution of an inverse problem by the optimal-control method implies having to deal with the solution of a differential algebraic boundary-value problem defined over the whole maneuver interval. Discretization by FETs in turn requires the solution of a nonlinear global problem on a given mesh. The system of discrete equations is obtained by assembling the contributions from each element and appending the other boundary and constraint conditions. Although the resulting matrices are banded and highly sparse, the desire for very quick response times and high numerical performance calls for efficient acceleration techniques.

Received 21 June 1999; revision received 30 March 2000; accepted for publication 2 April 2000.

*Riceratore, Dipartimento di Ingegneria Aerospaziale, Via La Masa 34, 20158 Milano, Italy; Carlo.Bottasso@polimi.it.

†Graduate Student, Dipartimento di Ingegneria Aerospaziale, Via La Masa 34, 20158 Milano, Italy.

It is well known that, for smooth problems, *p* adaption yields fast convergence to the desired level of accuracy. Unfortunately, raising the order of the method requires a solution of increasingly complex and expensive discrete operators. A way to circumvent this problem is represented by the deferred-correction technique. The basic idea of deferred correction is to keep the size of the discrete operator fixed, while improving its accuracy through clever, cheap estimates of the local discretization error.

In this work we develop a deferred-correction procedure for the FET formulation of optimal control. Deferred correction has been extensively studied in the context of global RK methods for boundary-value problems.[21–24] Here we adapt similar ideas to FETs. The computation of the correction terms is obtained element by element, in the sense that it does not require the solution of a global problem. This results in a particularly efficient procedure. Our current implementation gives uniform *p* refinement over the whole mesh. Future investigations will study the possibility of applying selected local corrections based on error estimates, a potential way of achieving further numerical efficiency through local *p* adaption.

The procedure is tested on some representative numerical simulations of fixed and rotating wing aircrafts. The method is formulated in such a way as to be completely independent of the particular type of vehicle being studied and of the particular maneuver being simulated. It allows one to deal with coupled nonlinear inertial and aerodynamic models with no particular difficulty. This would seem to be a desirable characteristic of any versatile simulation tool.

Boundary-Value Problems

A generic boundary-value problem can be defined in terms of a system of first-order ordinary differential equations (ODEs),

$$\dot{\boldsymbol{y}} = \boldsymbol{g}(\boldsymbol{y}, \boldsymbol{z}, t) \tag{1a}$$

possibly subjected to the algebraic constraints

$$\boldsymbol{a}(\boldsymbol{y}, \boldsymbol{z}, t) = 0 \tag{1b}$$

where $(\dot{\bullet}) = \mathrm{d}\bullet/\mathrm{d}t$, $\boldsymbol{y} \in \mathbb{R}^Y$, $\boldsymbol{z} \in \mathbb{R}^Z$, $t \in \mathbb{R}$, $\boldsymbol{g}: \mathbb{R}^Y \times \mathbb{R}^Z \times \mathbb{R} \to \mathbb{R}^Y$, $\boldsymbol{a}: \mathbb{R}^Y \times \mathbb{R}^Z \times \mathbb{R} \to \mathbb{R}^Z$. Here $I = [0, T]$ is the time domain. Suitable boundary and additional constraint conditions are given as

$$\boldsymbol{C}[\boldsymbol{y}(0), \boldsymbol{y}(T), T] = 0 \tag{1c}$$

This format covers a wide range of applications, in particular optimal-control problems with or without unknown terminal time and path constraints.

Optimal Control Problems

Let us consider a dynamical system with n states $\boldsymbol{x}$ and m controls $\boldsymbol{u}$, governed by the following set of ODEs:

$$\dot{\boldsymbol{x}} = \boldsymbol{f}(\boldsymbol{x}, \boldsymbol{u}, t) \tag{2}$$

The q constraints on $\boldsymbol{x}$ at 0 and T are given as

$$\boldsymbol{\psi}[\boldsymbol{x}(0), \boldsymbol{x}(T), T] = 0 \tag{3}$$

Boundary conditions on the states can be included in this term. A performance index J is defined as

$$J := \phi[\boldsymbol{x}(0), \boldsymbol{x}(T), T] + \int_0^T L[\boldsymbol{x}(t), \boldsymbol{u}(t), t]\,\mathrm{d}t \tag{4}$$

The problem is to find $\boldsymbol{u}$ and $\boldsymbol{x}$ that, satisfying the equations of motion and the constraints, minimize J. Adjoining the system ODEs (2) and constraints (3) with multipliers $\boldsymbol{\lambda}$ and $\boldsymbol{\nu}$ to J, we get

$$\bar{J} = \phi + \boldsymbol{\nu} \cdot \boldsymbol{\psi} + \int_0^T [L + \boldsymbol{\lambda} \cdot (\boldsymbol{f} - \dot{\boldsymbol{x}})]\,\mathrm{d}t \tag{5}$$

The stationarity of $\bar{J}$ yields the optimum control differential algebraic equations

$$\dot{\boldsymbol{x}} = \boldsymbol{f}(\boldsymbol{x}, \boldsymbol{u}, t) \tag{6a}$$

$$\dot{\boldsymbol{\lambda}} = -\frac{\partial H^T}{\partial \boldsymbol{x}} = -\frac{\partial L^T}{\partial \boldsymbol{x}} - \frac{\partial \boldsymbol{f}^T}{\partial \boldsymbol{x}}\boldsymbol{\lambda} \tag{6b}$$

$$0 = \frac{\partial H^T}{\partial \boldsymbol{u}} = \frac{\partial L^T}{\partial \boldsymbol{u}} + \frac{\partial \boldsymbol{f}^T}{\partial \boldsymbol{u}}\boldsymbol{\lambda} \tag{6c}$$

subjected to the boundary conditions

$$\boldsymbol{\lambda}(0) = -\left(\frac{\partial \Phi}{\partial \boldsymbol{x}}\right)^T_{t=0} \tag{7a}$$

$$\boldsymbol{\lambda}(T) = \left(\frac{\partial \Phi}{\partial \boldsymbol{x}}\right)^T_{t=T} \tag{7b}$$

$$\left(L + \boldsymbol{\lambda} \cdot \boldsymbol{f} + \frac{\partial \Phi}{\partial t}\right)_{t=T} = 0 \tag{7c}$$

$$\boldsymbol{\psi}[\boldsymbol{x}(0), \boldsymbol{x}(T), T] = 0 \tag{7d}$$

H is the system Hamiltonian, defined as

$$H := L + \boldsymbol{\lambda} \cdot \boldsymbol{f} \tag{8}$$

whereas function Φ is defined as

$$\Phi := \phi + \boldsymbol{\nu} \cdot \boldsymbol{\psi} \tag{9}$$

This problem follows within the definition of the general problem of Eqs. (1a–1c) and results in an index-one differential algebraic boundary-value problem. Conceptually minor alterations to this basic framework allow us to treat problems with interior point constraints, possibly at unknown intermediate times, and multiphase problems.[25]

Finite-Element-in-Time Methods

We select a mesh π for the solution of Eqs. (1a–1c), partitioning I according to

$$\pi\colon 0 = t_1 < t_2 < \cdots < t_{N+1} = T \tag{10}$$

and we let $h_n := t_{n+1} - t_n$. We consider global methods,[26] that is, methods that produce an approximate solution representation over the entire interval of interest. In the terminology of the finite-element method, these procedures assemble the equations over the whole interval. Alternative strategies are based on the solution of corresponding initial value problems, for example shooting and related techniques. A general reference on these topics is Ref. 26.

A general framework that unifies most known FET formulations was first proposed in Ref. 27, and it was discussed again in Ref. 17. It turns out that FET methods can be divided in two families: methods that are "symmetric" with respect to the direction of time, and methods that are not, and therefore provide some form of information "upwinding." Here we are interested in the former methods, termed in Ref. 27 the bi-discontinuous (BD) FETs; the latter, the singly discontinuous (SD) FETs, are mostly suited to the integration of large sets of equations resulting from the semidiscretization of partial differential equations (PDEs). Further background information on these and related methods can be found in the references cited in Ref. 20.

FET methods are based on the approximation of a weak form of Eqs. (1a–1c):

$$\int_I [\boldsymbol{v} \cdot (\dot{\boldsymbol{y}} - \boldsymbol{g}) + \boldsymbol{w} \cdot \boldsymbol{a}]\,\mathrm{d}t + \boldsymbol{\theta} \cdot \boldsymbol{C} = 0 \tag{11}$$

In practice, one seeks a solution that satisfies in a weak sense Eqs. (1a), (1b), and the boundary conditions (1c). Integration by parts of the first term of Eq. (11) yields

$$\int_I (\dot{\boldsymbol{v}} \cdot \boldsymbol{y} + \boldsymbol{v} \cdot \boldsymbol{g} - \boldsymbol{w} \cdot \boldsymbol{a})\,\mathrm{d}t = \boldsymbol{v} \cdot \boldsymbol{y}|_{\partial I} + \boldsymbol{\theta} \cdot \boldsymbol{C} \tag{12}$$

where ∂I is the boundary of I.

Under certain circumstances, weak forms (11) and (12) can be given a variational interpretation; see, for example, Ref. 17. This is also the point of view given in Ref. 9.

The approximation of Eq. (12) is developed as follows. We construct finite-dimensional trial function spaces Y^h, Z^h as

$$Y^h := \left\{\boldsymbol{y}^h \in \left[\mathcal{P}^{k_y}(I_n)\right]^Y\right\}, \qquad Z^h := \left\{\boldsymbol{z}^h \in \left[\mathcal{P}^{k_z}(I_n)\right]^Z\right\} \tag{13a}$$

and test function spaces V^h, W^h as

$$V^h := \left\{\boldsymbol{v}^h \in \left[\mathcal{P}^{k_v}(I_n)\right]^Y\right\}, \qquad W^h := \left\{\boldsymbol{w}^h \in \left[\mathcal{P}^{k_w}(I_n)\right]^Z\right\} \tag{13b}$$

Here $\mathcal{P}^k$ denotes the space of the kth-order polynomials. Within the nth time element, the finite-element trial solutions are defined as

$$\boldsymbol{y}^h(t) := \begin{cases} \boldsymbol{y}^n, & \tau = 0 \\ \sum_{i=1}^{k_y+1} s_i^{k_y}(\tau)\boldsymbol{y}_i, & 0 < \tau < 1 \\ \boldsymbol{y}^{n+1}, & \tau = 1 \end{cases} \tag{14a}$$

$$\boldsymbol{z}^h(t) := \sum_{i=1}^{k_z+1} s_i^{k_z}(\tau)\boldsymbol{z}_i, \qquad 0 < \tau < 1 \tag{14b}$$

and the weighting functions are given as

$$\boldsymbol{v}^h(t) := \sum_{i=1}^{k_v+1} s_i^{k_v}(\tau)\boldsymbol{v}_i, \qquad 0 \le \tau \le 1 \tag{14c}$$

$$\boldsymbol{w}^h(t) := \sum_{i=1}^{k_w+1} s_i^{k_w}(\tau)\boldsymbol{w}_i, \qquad 0 < \tau < 1 \tag{14d}$$

with $\tau = (t - t_n)/(t_{n+1} - t_n)$. Here $\boldsymbol{y}_i$, $\boldsymbol{z}_i$, $\boldsymbol{v}_i$, and $\boldsymbol{w}_i$ are the vectors of nodal unknowns and test functions for node i. Clearly, the $\boldsymbol{y}_i, \boldsymbol{z}_i$ depend on n, but this dependence is not reflected in the notation. $s_i^{k_y}(\tau)$, $s_i^{k_z}(\tau)$, $s_i^{k_v}(\tau)$, and $s_i^{k_w}(\tau)$ are the finite-element shape functions of order k_y, k_z, k_v, and k_w, respectively, for node i.

Note that, from Eq. (14a), the trial solutions $\boldsymbol{y}^h$ are continuous within each time element, but discontinuous across the interface of the elements, namely at times $t_1, t_2, \ldots, t_{N+1}$, where we have the discrete boundary values $\boldsymbol{y}^1, \boldsymbol{y}^2, \ldots, \boldsymbol{y}^{N+1}$. Note then, from Eq. (14b), that also the trial solutions $\boldsymbol{z}^h$ are discontinuous across the element interfaces, but in this case there are no discrete boundary values at the boundary times. However, these values can be computed a posteriori so that the solution lies on the manifold, using

$$\boldsymbol{a}(\boldsymbol{y}^{n+1}, \boldsymbol{z}^{n+1}, t_{n+1}) = 0 \tag{15}$$

In conclusion, we are looking for solutions $\boldsymbol{y}^h \in Y^h$, $\boldsymbol{z}^h \in Z^h$ that satisfy

$$\int_{I_n} [\dot{\boldsymbol{y}}^h \cdot \boldsymbol{y}^h + \boldsymbol{v}^h \cdot \boldsymbol{g}(\boldsymbol{y}^h, \boldsymbol{z}^h, t) - \boldsymbol{w}^h \cdot \boldsymbol{a}(\boldsymbol{y}^h, \boldsymbol{z}^h, t)]\,\mathrm{d}t = \boldsymbol{v}^h \cdot \boldsymbol{y}^h|_{\partial I_n}$$

$$n = 1, \ldots, N \tag{16}$$

for all $\boldsymbol{v}^h \in V^h, \boldsymbol{w}^h \in W^h$. We choose for simplicity to drop the boundary condition term $\boldsymbol{\theta} \cdot \boldsymbol{C}$ from the following discussion because it does not require discretization. Furthermore, for a lighter notation, we omit in the next pages the superscript $(\bullet)^h$.

An inspection of Eq. (16) leads to the following choice for the order of the test and trial finite-element shape functions:

$$k_y = k_z = k_w = k_v - 1 \tag{17}$$

Finite-Element-in-Time Methods for Optimal-Control Problems

Reference 9 developed a numerical FET procedure for optimal-control problems, based on a direct discretization of the first variation of the performance index. This is a specialization of the above-presented formulation for generic boundary-value index-one differential algebraic problems. Reference 28 developed an hp-FET procedure for generic two-point boundary-value problems, which also falls within the above-discussed framework. Reference 16 shows that the procedure in both cases is equivalent to the use of a global, implicit RK scheme. This result is valid for the p version of the method, that is, for arbitrarily high order. The analysis shows that the quadrature rule used for evaluating the integrals in the weak form plays a major role, in practice determining the algorithmic properties of the resulting FET scheme. Using the Gauss, Lobatto and Radau–Left quadrature rules, one obtains FETs that correspond to the Kuntzmann–Butcher (Gauss), Lobatto IIIB, and Radau IA RK schemes, respectively.

Deferred Correction

Iterated deferred correction is widely used for the efficient numerical solution of boundary-value problems, because it allows high-order formulas to be implemented at reasonable computational costs.

Let us consider a boundary-value problem, and let ϕ_p be a p-order method used for its solution. We have

$$\phi_p(\boldsymbol{\eta}_\pi) = 0 \tag{18}$$

where $\boldsymbol{\eta}_\pi$ is the numerical solution on mesh π that approximates the restriction of the exact solution $\boldsymbol{\eta}$ to π, indicated as $\Delta\boldsymbol{\eta}$. The local discretization error $\boldsymbol{\tau}(\boldsymbol{\eta})$ is defined as

$$\boldsymbol{\tau}(\boldsymbol{\eta}) := \phi_p(\Delta\boldsymbol{\eta}) \tag{19}$$

It is clear that, knowing $\boldsymbol{\tau}(\boldsymbol{\eta})$ we could solve Eq. (19) to get the exact solution. The basic idea of deferred correction is to estimate $\boldsymbol{\tau}(\boldsymbol{\eta})$ through some operator $\boldsymbol{\epsilon}$, and to solve

$$\phi_p(\bar{\boldsymbol{\eta}}_\pi) = \boldsymbol{\epsilon}(\boldsymbol{\eta}_\pi) \tag{20}$$

where $\bar{\boldsymbol{\eta}}_\pi$ is now a better approximation to $\Delta\boldsymbol{\eta}$ than $\boldsymbol{\eta}_\pi$.

Skeel[29] has given the following fundamental order result for $\bar{\boldsymbol{\eta}}_\pi$.

Theorem 1: Consider a stable numerical method ϕ and the following conditions for Eqs. (18) and (20).

1) $\|\boldsymbol{\eta}_\pi - \Delta\boldsymbol{\eta}\| = \mathcal{O}(h^p)$
2) $\|\boldsymbol{\epsilon}(\Delta\boldsymbol{\eta}) - \phi(\Delta\boldsymbol{\eta})\| = \mathcal{O}(h^{p+r})$
3) $\|\boldsymbol{\epsilon}(\Delta\boldsymbol{\zeta})\| = \mathcal{O}(h^r)$

for arbitrary functions $\boldsymbol{\zeta}$ with at least r continuous derivatives. Then, it follows that

$$\|\bar{\boldsymbol{\eta}}_\pi - \Delta\boldsymbol{\eta}\| = \mathcal{O}(h^{r+p})$$

Since the seminal work of Fox,[30] the method has evolved considerably. Reference 31 proposed using the following general approach for defining $\boldsymbol{\epsilon}$:

$$\phi_p(\boldsymbol{\eta}_\pi) = 0 \tag{21a}$$

$$\phi_p(\bar{\boldsymbol{\eta}}_\pi) = \phi_p(\boldsymbol{\eta}_\pi) - \phi_{p+r}(\boldsymbol{\eta}_\pi) \tag{21b}$$

Cash has used mono-implicit[21] and Lobatto[23] RK formulas, obtaining variable-order deferred-correction schemes.

Deferred-Correction and Finite-Element-in-Time Methods

Iterated deferred corrections can be used to accelerate FET procedures. We use the approach sketched in Eqs. (21a) and (21b) and adapt it to the FET framework.

An initial order p solution is computed by solving the global problem

$$\mathbb{A}_{n=1}^{N} \left\{ \int_{I_n} [\dot{\boldsymbol{v}}_p \cdot \boldsymbol{y}_p + \boldsymbol{v}_p \cdot \boldsymbol{g}(\boldsymbol{y}_p, \boldsymbol{z}_p, t) - \boldsymbol{w}_p \cdot \boldsymbol{a}(\boldsymbol{y}_p, \boldsymbol{z}_p, t)]\, \mathrm{d}t - \boldsymbol{v}_p \cdot \boldsymbol{y}_p|_{\partial I_n} \right\} = 0 \tag{22}$$

obtained by assembling the elemental contributions (16) over the whole interval. The subscript $(\bullet)_p$ indicates the order of the method adopted, and $\mathbb{A}(\bullet)_{n=1}^{N}$ is the assembly operator for elements from 1 through N.

As a second step, n independent local initial value problems are solved by using an order $p+r$ method, with initial values $\boldsymbol{y}_p(t_n)$ given by Eq. (22):

$$\int_{I_n} [\dot{\boldsymbol{v}}_{p+r} \cdot \boldsymbol{y}_{p+r} + \boldsymbol{v}_{p+r} \cdot \boldsymbol{g}(\boldsymbol{y}_{p+r}, \boldsymbol{z}_{p+r}, t) - \boldsymbol{w}_{p+r} \cdot \boldsymbol{a}(\boldsymbol{y}_{p+r}, \boldsymbol{z}_{p+r}, t)]\, \mathrm{d}t = \boldsymbol{v}_{p+r} \cdot \boldsymbol{y}_{p+r}|_{t=t_{n+1}} - \boldsymbol{v}_{p+r} \cdot \boldsymbol{y}_p|_{t=t_n}, \qquad n = 1, \ldots, N \tag{23}$$

These local subproblems yield the values $\boldsymbol{y}_{p+r}(t_{n+1})$ that are used in the next step for constructing the corrections.

Finally, a corrected order $p+r$ solution is computed by solving the global problem

$$\mathbb{A}_{n=1}^{N} \left\{ \int_{I_n} [\dot{\boldsymbol{v}}_p \cdot \bar{\boldsymbol{y}}_{p+r} + \boldsymbol{v}_p \cdot \boldsymbol{g}(\bar{\boldsymbol{y}}_{p+r}, \bar{\boldsymbol{z}}_{p+r}, t) - \boldsymbol{w}_p \cdot \boldsymbol{a}(\bar{\boldsymbol{y}}_{p+r}, \bar{\boldsymbol{z}}_{p+r}, t)]\, \mathrm{d}t - \boldsymbol{v}_p \cdot (\bar{\boldsymbol{y}}_{p+r} - \boldsymbol{\epsilon})|_{t=t_{n+1}} + \boldsymbol{v}_p \cdot \bar{\boldsymbol{y}}_{p+r}|_{t=t_n} \right\} = 0 \tag{24}$$

with

$$\boldsymbol{\epsilon} = \boldsymbol{y}_{p+r} - \boldsymbol{y}_p \tag{25}$$

Alternative strategies for evaluating the error are possible in the FET framework, as explored, for example, in Ref. 20.

Validation of the Numerical Procedure

Here we validate the proposed numerical procedure, solving two simple optimal-control problems whose solution is given in closed form in Ref. 25.

We consider a particle of mass m, moving in the plane x–y and subjected to a constant acceleration a. The velocity components of the particle along x and y are noted u and v, respectively. The angle β between the acceleration vector and x represents the control variable of the problem. In the first example, we want to transfer the particle to a path parallel to the x axis, a distance h away, in a given time T, arriving with the maximum possible value of u. In the second example, we want to transfer in minimum time the same particle to the same trajectory, but with given final velocity U.

In both cases, we start generating a first solution with a FET method of order p. The solution is then improved by using the deferred-correction technique based on a formula of order $p+2$. In all cases, numerical quadrature is performed by using the Gauss–Legendre rule. We consider the case in which the number of quadrature points is the same as the number of finite-element nodes. This ensures that the resulting solution is equivalent to the one obtained by using a Kuntzmann–Butcher RK scheme, which implies interesting numerical properties.[17] The local mesh size h_n is selected as

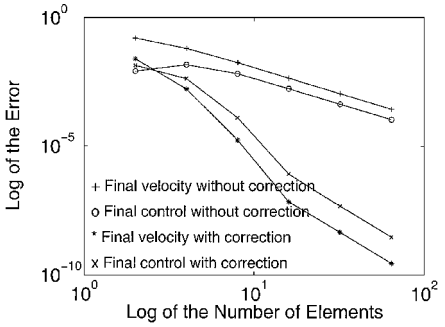

Fig. 1 Transfer to a rectilinear path: fixed final time, second-order base scheme with and without correction. Solution error vs number of time elements.

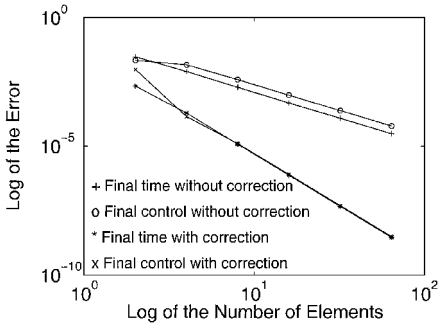

Fig. 2 Transfer to a rectilinear path: free final time, second-order base scheme with and without correction. Solution error vs number of time elements.

$(T - t_0)/N$ for all values of n. The solution is based on the Newton–Raphson method, with an exact tangent matrix. The control values at the element interfaces are recovered by using the optimal condition (6c).

For the first example, we set $h = 100$ m, $T = 20$ s, and $\beta_0 = 75$ deg. For the second example, we set $h = 100$ m, $U = 10$ m/s, and an initial control value $\beta_0 = 60$ deg.

For the fixed final time problem, Fig. 1 gives the percent error between the computed and exact final values of the control and of the particle velocity, as a function of the number of time steps. The second-order accurate scheme ($k_y = 0$) was used for the base solution, and the figure shows that the corrected solution achieves an order of four. We also tested the base fourth-order scheme ($k_y = 1$), obtaining an order of six in the corrected solution.

For the free final time problem, Fig. 2 gives the percent error between the numerical and analytical solutions of the final control and time, as a function of the number of time steps. The base scheme used was the second-order one ($k_y = 0$), and the figure shows that the corrected solution is of the order of four. Correction of the base fourth-order scheme ($k_y = 1$) gave an order-six method even for this example.

These results show that the proposed deferred-correction scheme allows one to obtain an order $p + 2$ solution, correcting a base p scheme with a $p + 2$ method.

Inverse Flight Simulation

Here we study the application of the proposed method to the inverse simulation of flight. The first two examples presented in the following pages analyze the fixed wing case; the third and fourth ones regard the rotating wing case.

The state equations are the classical equations of flight mechanics[32] and are written as

$$\dot{u} = -qw + rv - g\sin\theta + X^A/m \tag{26a}$$

$$\dot{v} = -ru + pw + g\cos\theta\sin\phi + Y^A/m \tag{26b}$$

$$\dot{w} = -pv + qu + g\cos\theta\cos\phi + Z^A/m \tag{26c}$$

$$\dot{p} = [(I_x - I_y + I_z)/J]I_{xz}pq - \left[\left(I_z^2 - I_yI_z + I_{xz}^2\right)/J\right]qr + I_{xz}N^A/J + I_zL^A/J \tag{27a}$$

$$\dot{q} = (I_{xz}/I_y)(r^2 - p^2) + [(I_z - I_x)/I_y]rp + M^A/I_y \tag{27b}$$

$$\dot{r} = -[(I_x - I_y + I_z)/J]I_{xz}qr + \left[\left(I_x^2 - I_yI_x + I_{xz}^2\right)/J\right]pq + I_xN^A/J + I_{xz}L^A/J \tag{27c}$$

with $J = I_xI_z - I_{xz}^2$,

$$\dot{y} = \sin\psi\cos\theta u + (\sin\psi\sin\theta\sin\phi + \cos\psi\cos\phi)v + (\sin\psi\sin\theta\cos\phi - \cos\psi\sin\phi)w \tag{28a}$$

$$\dot{z} = -\sin\theta u + \cos\theta\sin\phi v + \cos\theta\cos\phi w \tag{28b}$$

$$\dot{\phi} = p + \sin\phi\tan\theta q + \cos\phi\tan\theta r \tag{29a}$$

$$\dot{\theta} = \cos\phi q - \sin\phi r \tag{29b}$$

$$\dot{\psi} = (\sin\phi/\cos\theta)q + (\cos\phi/\cos\theta)r \tag{29c}$$

Functions $L(\boldsymbol{x}, \boldsymbol{u}, t)$ and $\phi(\boldsymbol{x}, t)$, which define the performance index, are chosen as

$$L = \tfrac{1}{2}(\mathrm{d}A^2 + \mathrm{d}E^2 + \mathrm{d}R^2 + \mathrm{d}T^2) \tag{30a}$$

$$\phi[\boldsymbol{x}(t), t] = 0 \tag{30b}$$

$\mathrm{d}A$, $\mathrm{d}E$, $\mathrm{d}R$, and $\mathrm{d}T$ are the control deflections from the reference flight conditions. For the fixed wing case, A is the average aileron deflection, E is the elevator deflection, R is the rudder deflection, and T is a quantity related to the throttle angular position. For the rotating wing case, A is the later cyclic, E the longitudinal cyclic, R the tail collective, and T the main rotor collective.

In order to prescribe the selected maneuvers, the time histories of the roll angle ϕ, the z coordinate of the center of mass of the vehicle, and the v velocity component are imposed as constraints. The constraints are derived with respect to time a sufficient number of times in order to get explicit dependence on the controls (reduction to index-one form). Another constraint ensures that a straight level flight path is recovered at the termination of the maneuver.

In practice, through this process we will determine, among all the possible solutions to the inverse problem of flight, the one that minimizes the control deflections and satisfies all the path and boundary constraints. It is clear that many other definitions of the performance index and of the constraints are possible within this same framework. For example, one could easily analyze minimum time maneuvers. Or one might want to consider constant throttle maneuvers, because this control can be considerably "slower" than the others. Many other choices are possible, depending on the particular problem being studied; these choices are, however, easily handled in the context of the general optimal control theory.

For all simulations reported in the following paragraphs, the base solution is the second-order scheme denoted by $k_y = 0$ and Gauss quadrature, and the nonlinear discrete equations are solved by using the Newton–Raphson scheme with an exact tangent. For the fighter simulations, the Levenberg–Marquardt algorithm was used for its greater robustness.

Fixed Wing Case

We consider an A-4D in symmetric straight level flight at 4572 m, at a speed of $U_0 = 193.24$ m/s. The aircraft data are taken from Ref. 33.

The problem can be simplified by imposing that the u velocity component is constant and equal to U_0. L can then be redefined in this case as $L = \frac{1}{2}(\mathrm{d}A^2 + \mathrm{d}E^2 + \mathrm{d}R^2)$, and the thrust values can be recovered a posteriori once the solution has been computed.

360 Degree Roll

The aircraft must complete a 360-deg roll in T seconds. The constraint reads

$$\phi - (2\pi/16)[\cos(3\pi t/T) - 9\cos(\pi t/T) + 8] = 0 \qquad (31)$$

The straight level flight condition at the end of the maneuver is imposed as

$$\psi[\boldsymbol{x}(T), T] = (y, z, v, w, \theta, \psi, q, r)^T = 0 \qquad (32)$$

We set $T = 6$ s. The simulation results are given in Figs. 3 and 4. Note that the trajectory in the y–z plane remains confined to a region close to the origin. The vehicle starts moving in the positive y direction, and then it moves in the opposite negative direction. This is accompanied first by a gain in altitude, followed by a return to the original z value. The deflection of the control surfaces is always

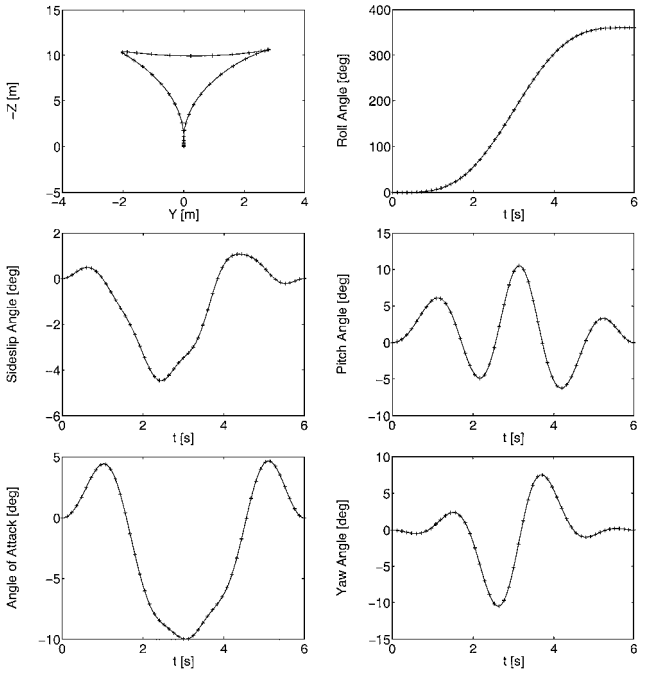

Fig. 3 360-deg roll maneuver of an A-4D aircraft.

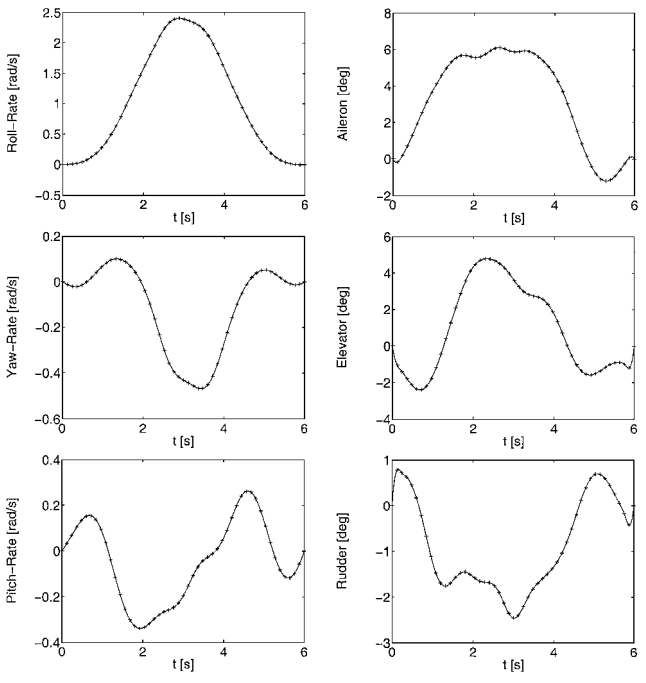

Fig. 4 360-deg roll maneuver of an A-4D aircraft.

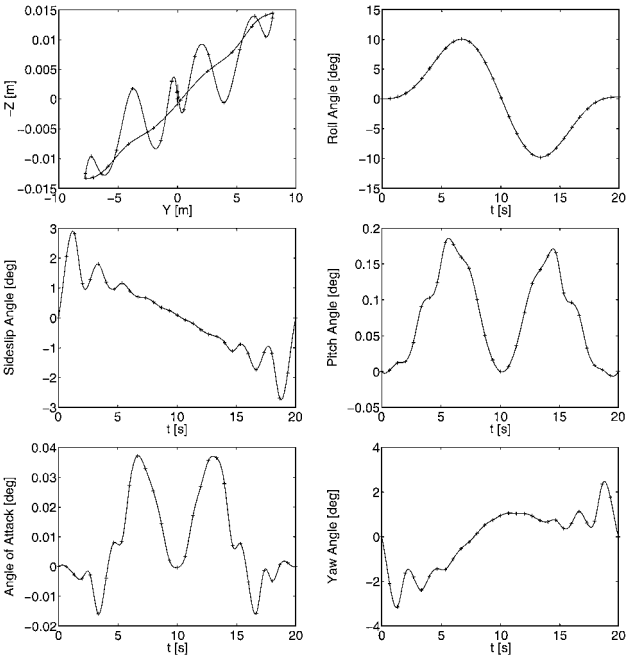

Fig. 5 Prescribed bank-to-bank maneuver of an A-4D aircraft.

contained to acceptable limits. The aileron deflection maintains the same sign throughout the maneuver, and this is due to the need to rotate the aircraft about the roll axis always in the same direction. The same example was analyzed in Ref. 8. Although we used a different inertial model of the vehicle and a different approach for enforcing the constraints, the results are in close agreement.

Bank-to-Bank Maneuver

The aircraft must complete a maneuver characterized by the following time history of roll:

$$\phi - \left(\pi/27\sqrt{3}\right)[-\sin(4\pi t/T) + 2\sin(2\pi t/T)] = 0 \qquad (33a)$$

and by a constant altitude

$$z = 0 \qquad (33b)$$

ψ is in this case selected as

$$\psi[\boldsymbol{x}(T), T] = (y, v, w, \psi, q, r)^T = 0 \qquad (34)$$

Figures 5 and 6 give the time histories of the states and controls, computed for a maneuver duration of $T = 20$ s and using a grid of 30 finite elements. The flight path is denoted by an almost constant altitude. First, the vehicle moves toward the left and then toward the right, because of the negative rotation about the yaw axis. Even in this case, the deflection of all the control surfaces is limited. The deflections of aileron and rudder are finalized to the achievement of the desired time history of roll, whereas the deflection of the elevator is almost null. This is a result of the limited movement about the pitch axis, implied by the imposition of the fixed altitude constraint. A similar example was analyzed in Ref. 8.

Rotating Wing Case

Rotating wing inverse problems are analyzed, with results similar to the ones here reported, in Refs. 2 and 5. Here we consider a UH-60 helicopter in straight symmetric level flight at sea level, at a speed of $U_0 = 35$ m/s. The aircraft data are taken from Ref. 34.

The problem can be simplified by eliminating the y component of the position vector and the ψ orientation parameter. Both states can be recovered a posteriori, once the solution has been obtained.

Hurdle Hop

The helicopter must complete a hurdle-hop maneuver in T seconds, with null sideslip, simulating a terrain-following maneuver.

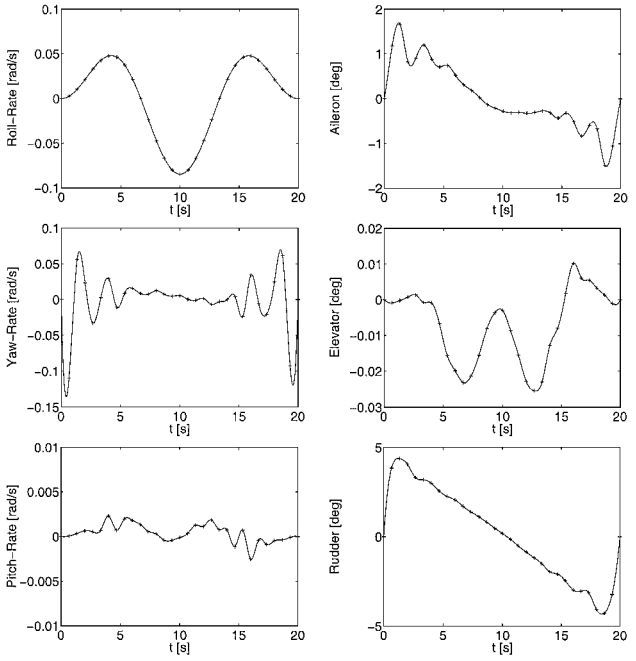

Fig. 6 Prescribed bank-to-bank maneuver of an A-4D aircraft.

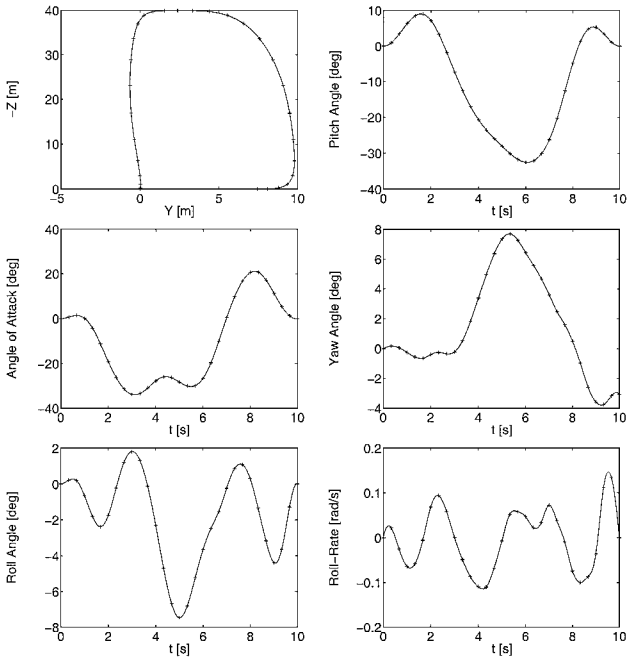

Fig. 7 Hurdle-hop maneuver of a UH-60 helicopter.

The constraints read

$$z + (40/16)[\cos 3\pi(2t/T) - 9\cos\pi(2t/T) + 8] = 0 \qquad (35a)$$

and

$$v = 0 \qquad (35b)$$

ψ is given by

$$\psi = (u - 35, w, \phi, p, q, r)^T = 0 \qquad (36)$$

We select $T = 10$ s and use 30 time elements within this interval. The results are shown in Figs. 7 and 8. Note how the helicopter moves toward the positive values of y during the maneuver. The tail collective, as expected, closely follows the time history of the main rotor collective.

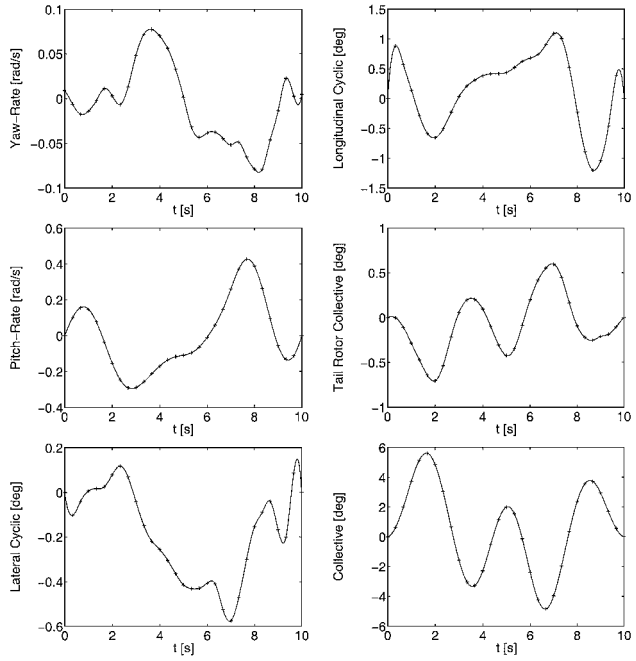

Fig. 8 Hurdle-hop maneuver of a UH-60 helicopter.

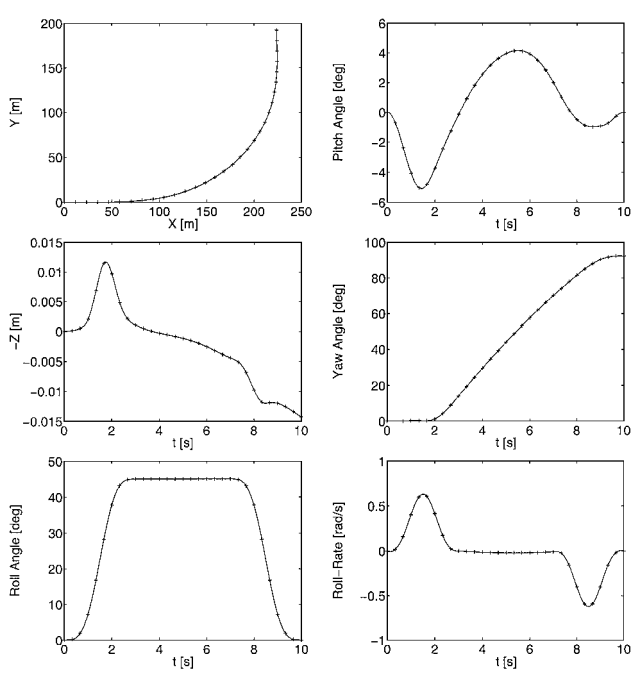

Fig. 9 Level turn maneuver of a UH-60 helicopter.

Level Turn

The helicopter must perform a level turn of 90 deg in T seconds, with given roll time history and null sideslip. The constraints read in this case

$$\phi - (\pi/64)[\cos 3\pi(t/3) - 9\cos\pi(t/3) + 8] = 0, \qquad 0 \le t \le 3 \text{ s}$$

$$\phi - \pi/4 = 0, \qquad 3 < t < 7 \text{ s}$$

$$\phi - (\pi/4)\Big(1 - \tfrac{1}{16}\big\{\cos 3\pi[(t-7)/3] - 9\cos\pi[(t-7)/3] + 8\big\}\Big) = 0, \qquad 7 \le t \le 10 \text{ s} \qquad (37a)$$

$$z = 0 \qquad (37b)$$

$$v = 0 \qquad (37c)$$

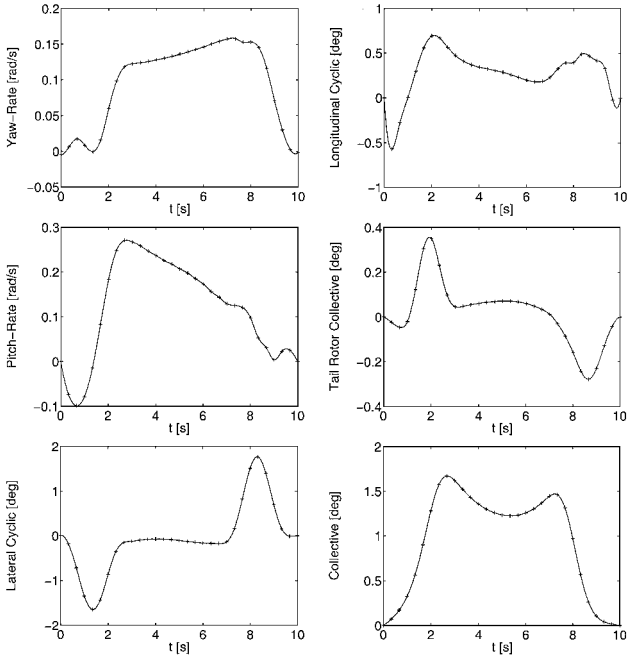

Fig. 10 Level turn maneuver of a UH-60 helicopter.

ψ is given by

$$\psi[\boldsymbol{x}(T), T] = (u - 35, w, q, r)^T = 0 \tag{38}$$

We set $T = 10$ s and use 30 time elements. The results are presented in Figs. 9 and 10. The helicopter realizes the imposed turn, with negligible change in altitude. The main rotor collective generates the force required for curving the flight trajectory. The later cyclic is first negative and then positive, allowing the forces generated by the rotor to be oriented. Its time history is analogous, although with a different sign, to the time history of the tail rotor collective.

To assess once more the order increase achieved by means of the presented deferred-correction technique, we solved the same problem on a mesh of 50 time elements. The slope of the roll error versus the number of elements was found to be equal to -2.23 for the base scheme, whereas it rose to the value of -4.79 for the deferred-correction method.

Conclusions

We have developed a deferred-correction optimal-control FET procedure for the solution of inverse problems in flight mechanics. Optimal-control theory gives a solid background for the study of this class of problems. FETs give a strikingly simple way of deriving an efficient numerical scheme from the basic variational principles of the classic theory. Furthermore, FETs are in reality global implicit RK schemes, which are among the most studied, well understood, and trusted numerical technologies available today. All these features give a simple, straightforward method that is also highly robust and flexible. Versatility and generality is a key point: the developed procedures can accommodate different models of flying vehicles and of their aerodynamic characteristics. The models adopted can then be tailored to the particular requirements of the analysis without the need to resort to new methods.

We have applied a deferred-correction acceleration technique to the basic FET procedure. This gives a uniform p-refinement method without requiring the computational costs associated with the solution of higher-order discrete operators. The implementation is based on an efficient element-by-element construction of the correction terms. Future investigations will have to address the implementation of local acceleration techniques, which could further enhance the method by locally p-refining the mesh only where needed by the features of the solution.

We have tested our numerical procedures with the help of simulations of both fixed and rotating wing aircrafts. The results obtained are encouraging, and they confirm the basic features of the proposed methodology. It is also clear that the same numerical technique is of general applicability, and it can be used unchanged for optimal-control problems other than the inverse problems of flight mechanics studied here.

References

[1]Kato, O., and Sugiura, I., "An Interpretation of Airplane General Motion and Control as Inverse Problem," *Journal of Guidance, Control, and Dynamics*, Vol. 9, No. 2, 1986, pp. 198–204.

[2]Thompson, D. G., and Bradley, R., "Development and Verification of an Algorithm for Helicopter Inverse Simulations," *Vertica*, Vol. 14, No. 2, 1990, pp. 185–200.

[3]Sentoh, E., and Bryson, A. E., "Inverse and Optimal Control for Desired Outputs," *Journal of Guidance, Control, and Dynamics*, Vol. 15, No. 3, 1992, pp. 687–691.

[4]Gao, C., and Hess, R. A., "Inverse Simulation of Large-Amplitude Aircraft Maneuvers," *Journal of Guidance, Control, and Dynamics*, Vol. 16, No. 4, 1993, pp. 733–737.

[5]Hess, R. A., and Gao, C., "A Generalized Algorithm for Inverse Simulation Applied to Helicopter Maneuvering Flight," *Journal of the American Helicopter Society*, Vol. 38, Oct. 1993, pp. 3–15.

[6]Matteis, G., Socio, L., and Leonessa, A., "Solution of Aircraft Inverse Problems by Local Optimization," *Journal of Guidance, Control, and Dynamics*, Vol. 8, No. 3, 1995, pp. 567–571.

[7]Borri, M., Bottasso, C. L., and Montelaghi, F., "A Numerical Approach to Inverse Flight Dynamics," *Journal of Guidance, Control, and Dynamics*, Vol. 20, No. 4, 1997, pp. 1–6.

[8]Lee, S., and Kim, Y., "Time-Domain Finite Element Method for Inverse Problem of Aircraft Maneuvers," *Journal of Guidance, Control, and Dynamics*, Vol. 20, No. 1, 1997, pp. 97–103.

[9]Hodges, D. H., and Bless, R. R., "Weak Hamiltonian Finite Element Method for Optimal Control Problems," *Journal of Guidance, Control, and Dynamics*, Vol. 14, No. 1, 1991, pp. 148–156.

[10]Hodges, D. H., Bless, R. R., Calise, A. J., and Leung, M., "Finite Element Method for Optimal Guidance of an Advanced Launch Vehicle," *Journal of Guidance, Control, and Dynamics*, Vol. 15, No. 3, 1992, pp. 664–671.

[11]Bless, R. R., and Hodges, D. H., "Finite Element Solution of Optimal Control Problems with State-Control Inequality Constraints," *Journal of Guidance, Control, and Dynamics*, Vol. 15, No. 4, 1992, pp. 1029–1032.

[12]Bless, R. R., Hodges, D. H., and Seywald, H., "Finite Element Method for the Solution of State-Constrained Optimal Control Problems," *Journal of Guidance, Control, and Dynamics*, Vol. 18, No. 5, 1995, pp. 1036–1043.

[13]Hodges, D. H., and Johnson, M. G. Jr., "Control Variables for Finite Element Solution of Missile Trajectory Optimization," *Journal of Guidance, Control, and Dynamics*, Vol. 18, No. 5, 1995, pp. 1208–1211.

[14]Warner, M. S., and Hodges, D. H., "Solving Optimal Control Problems Using hp-Version Finite Elements in Time," *Journal of Guidance, Control, and Dynamics*, Vol. 23, No. 1, 2000, pp. 86–94.

[15]Warner, M. S., and Hodges, D. H., "Treatment of Control Constraints in Finite Element Solution of Optimal Control Problems," *Journal of Guidance, Control, and Dynamics*, Vol. 22, No. 2, 1999, pp. 358–360.

[16]Bottasso, C. L., and Ragazzi, A., "Finite Element and Runge-Kutta Methods for Boundary-Value and Optimal Control Problems," *Journal of Guidance, Control, and Dynamics*, Vol. 23, No. 4, 2000, pp. 749–751.

[17]Bottasso, C. L., "A New Look at Finite Elements in Time: A Variational Interpretation of Runge-Kutta Methods," *Applied Numerical Mathematics*, Vol. 25, No. 4, 1997, pp. 355–368.

[18]Bader, G., and Ascher, U. M., "A New Basis Implementation for a Mixed Order Boundary Value ODE Solver," *SIAM Journal on Scientific and Statistical Computing*, Vol. 8, No. 4, 1987, pp. 483–500.

[19]Cash, J. R., Moore, G., and Wright, R. W., "An Automatic Continuation Strategy for the Solution of Singularly Perturbed Nonlinear Boundary Value Problems," *Journal of Computational Physics*, Vol. 122, No. 2, 1995, pp. 266–279.

[20]Estep, D., Hodges, D. H., and Warner, M. S., "Computational Error Estimation and Adaptive Error Control for a Finite Element Solution of Launch Vehicle Trajectory Problems," *SIAM Journal on Numerical Analysis* (to be published).

[21]Cash, J. R., "On the Numerical Integration of Nonlinear Two-Point Boundary Value Problems Using Iterated Deferred Corrections. Part 2: The Development and Analysis of Highly Stable Deferred Correction Formulæ," *SIAM Journal on Numerical Analysis*, Vol. 24, No. 4, 1988, pp. 862–882.

[22]Cash, J. R., and Wright, M. H., "A Deferred Correction Method for Nonlinear Two-Point Boundary Value Problems. Implementation and Numerical Evaluation," *SIAM Journal on Scientific and Statistical Computing*, Vol. 12, No. 4, 1991, pp. 971–989.

[23]Bashir-Ali, Z., Cash, J. R., and Silva, H. H. M., "Lobatto Deferred Correction for Stiff Two-Point Boundary Value Problems," *Computer and Mathematics with Applications*, Vol. 36, No. 10/12, 1998, pp. 59–69.

[24]Cash, J. R., "Runge-Kutta Methods for the Solution of Stiff Two-Point Boundary Value Problems," *Applied Numerical Mathematics*, Vol. 22, No. 1/3, 1996, pp. 165–177.

[25]Bryson, A. E., and Ho, Y.-C., *Applied Optimal Control—Optimization, Estimation, and Control*, Hemisphere, New York, 1975, Chaps. 2–3.

[26]Ascher, U. M., Mattheij, R. M. M., and Russell, R. D., *Numerical Solution of Boundary Value Problems for Ordinary Differential Equations*, Prentice–Hall, Englewood Cliffs, NJ, 1988.

[27]Borri, M., and Bottasso, C. L., "A General Framework for Interpreting Time Finite Element Formulations," *Computational Mechanics*, Vol. 13, 1993, pp. 133–142.

[28]Warner, M. S., and Hodges, D. H., "Solving Boundary-Value Problems Using hp-Version Finite Elements in Time," *International Journal for Numerical Methods in Engineering*, Vol. 43, No. 3, 1998, pp. 425–440.

[29]Skeel, R. D., "A Theoretical Framework for Proving Accuracy Results for Deferred Corrections," *SIAM Journal on Numerical Analysis*, Vol. 19, No. 1, 1982, pp. 171–196.

[30]Fox, L., "Some Improvements in the Use of Relaxation Methods for the Solution of Ordinary and Partial Differential Equations," *Proceedings of the Royal Society of London*, Series A 190, 1947, pp. 31–59.

[31]Lindberg, B., "Error Estimation and Iterative Improvement for Discretization Algorithms," *BIT*, Vol. 20, 1980, pp. 486–500.

[32]Etkin, B., *Dynamics of Atmospheric Flight*, Wiley, New York, 1972.

[33]Mc Ruer, D., Ashkenas, I., and Graham, D., *Aircraft Dynamics and Automatic Control*, Princeton Univ. Press, Princeton, NJ, 1973, pp. 700–706.

[34]Mc Lean, D., *Automatic Flight Control Systems*, Prentice–Hall, New York, 1990, pp. 482–483.